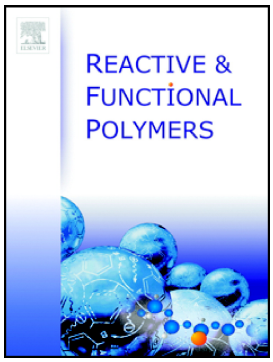

Synthesis and characterization of a novel inulin hydrogel crosslinked with pyromellitic dianhydride

Franklin Afinjuomo, Thomas G. Barclay, Yunmei Song, Ankitkumar Parikh, Nikolai Petrovsky, Sanjay Garg

PII: S1381-5148(18)30689-8
DOI: https://doi.org/10.1016/j.reactfunctpolym.2018.10.014
Reference: REACT 4153

To appear in: *Reactive and Functional Polymers*

Received date: 1 August 2018
Revised date: 18 October 2018
Accepted date: 28 October 2018

Please cite this article as: Franklin Afinjuomo, Thomas G. Barclay, Yunmei Song, Ankitkumar Parikh, Nikolai Petrovsky, Sanjay Garg , Synthesis and characterization of a novel inulin hydrogel crosslinked with pyromellitic dianhydride. React (2018), https://doi.org/10.1016/j.reactfunctpolym.2018.10.014

Synthesis and characterization of a novel inulin hydrogel crosslinked with pyromellitic dianhydride

Franklin Afinjuomo,[1] Thomas G. Barclay,[1] Yunmei Song,[1] Ankitkumar Parikh,[1] Nikolai Petrovsky,[2,3] Sanjay Garg[1]

[1] Centre for Pharmaceutical Innovation and Development, University of South Australia, Adelaide, South Australia 5001, Australia

[2] Vaxine Pty. Ltd., Adelaide, South Australia 5042, Australia

[3] Department of Endocrinology, Flinders University, Adelaide, South Australia 5042, Australia

*Corresponding Author. Telephone: (+61) 8 8302 1575 Email: Sanjay Garg @unisa.edu.au

Highlight

- A novel hydrogel was obtained by esterification between inulin and PMDA in a one-pot synthesis
- The physicochemical properties of the hydrogel were characterized using a range of techniques including Flory-Rehner theory to establish crosslinking density
- Hydrogels with different crosslinking density were obtained by varying the ratio of PMDA to inulin in the esterification
- The hydrogels demonstrated pH dependent swelling that was inversely proportional to the amount of PMDA

Keyword

Hydrogel

Inulin

Pyromellitic dianhydride

Crosslinking

pH dependent swelling

ABSTRACT

Smart hydrogels with pH and enzyme triggered release suitable for colon specific drug delivery were prepared by crosslinking inulin with pyromellitic dianhydride (PMDA) in a simple one pot synthesis. Back titration, Fourier transform infrared spectroscopy (FTIR) and ultraviolet spectrophotometry (UV) demonstrated that the hydrogel crosslinking reaction resulted in ester linkages and carboxylic acid groups and that the amount of the crosslinker in the hydrogel increased with increasing PMDA concentration in the crosslinking reaction. Thermal analysis and scanning electron microscopy (SEM) confirmed the chemical change by illustrating the hydrogels changed thermal properties and appearance compared to inulin. This hydrogel showed excellent swelling in water and the degree of swelling was inversely proportional to the cross-linking density, as determined using Flory-Rehner theory. Due to the presence of the carboxylic acid groups in the structure, the swelling was pH dependent, with significantly reduced swelling as acidity decreased from pH 7.4 to pH 1.2.

1. Introduction

Inulin is a natural fructan commonly found in plants such as chicory, dahlia, Jerusalem artichoke [1] as well as edible fruits and vegetables such as onion, leek, garlic and banana [2]. Inulin consists of linear chains of fructosyl groups linked by β(2→1) glycosidic bonds and terminated at the reducing end by an α-D-(2→1)-glucopyranoside ring (Figure 1) [3]. The widespread use of inulin in food and pharmaceutical industries can be ascribed to its desirable properties common to many polysaccharides such as biocompatibility, biodegradability, renewability and non-toxicity reflected in its Generally Recognized as Safe (GRAS) status granted by the Food and Drug Administration (FDA). Further, the multiple hydroxyl groups when combined with the unusually flexible backbone structure of inulin and its increased solubility compared to other polysaccharides means it is readily chemically modified, making it an adaptable platform for a variety of pharmaceutical functions. These include use as an excipient, protein stabilizer [4-8], drug dissolution enhancer [9, 10] vaccine adjuvant [11, 12] and cancer inhibitor [13-15] as well as for clinical measurement of kidney function [16, 17] lipid-lowering [18], glucose control [19], gastrointestinal tract treatments (dietary fibre, prebiotic, IBS and constipation) [20-22] and finally in drug delivery [23] including targeted colon delivery [24-26] and pulmonary delivery [27]

Similarly to many polysaccharides, the chemistry and structure of inulin allow physical or chemical crosslinking into tridimensional polymeric networks called hydrogels. These hydrogels are capable of soaking up large amounts of aqueous solution, such as physiological fluid and yet remain insoluble [28-31]. The excellent swelling ability, permeability and biodegradability make polysaccharide-based hydrogels ideal drug delivery vehicles. Several approaches for obtaining inulin hydrogels have been reported in the literature such as chemical modification of inulin with methacrylate groups using methacrylic anhydride or glycidyl methacrylates, followed by direct crosslinking through radical chemistry,[32] UV irradiation [33] and through linkers such as succinic anhydride (SA),[34] diacrylates[35] and a bis(methacrolylamino) azobenzene [36, 37]. Divinyl sulfone has also been used

directly as an inulin crosslinker [38] and succinic anhydride modified inulin was crosslinked with α,β-polyaspartylhydrazide using peptide coupling chemistry [39]. This crosslinking of inulin resulted in new biomaterials that were exploited for drug delivery and biomedical applications encapsulating various drug molecules such as ibuprofen [40], diflunisal [34], 2-methoxyestradiol [41], flutamide [42], prednisolone [36], oxytocin and glutathione [39] and also proteins including immunoglobulin G (IgG) [33], bovine serum albumin and lysozyme [26] and the latter two examples exploiting inulin's unique properties for delivery to the colon.

Inulin has great utility for colon delivery as it is not digestible to native human enzymes, but digested by bifidobacteria in the gut [26, 36, 43, 44] and so drug delivery platforms can be designed to degrade in the colon for drug release. Carboxylic acid groups have also been incorporated into the hydrogel through a reaction with succinic anhydride to improve the water swelling as well as conferring pH dependent swelling properties [45]. This translates to better drug loading and pH tuneable release, minimizing release under the acidic conditions in the stomach. Examples of this include the report by Castelli et al who synthesized inulin hydrogels with pH dependent swelling properties by modifying inulin with methacrylic anhydride and then succinic anhydride before UV crosslinking [34]. This synthesis method was time consuming employing multiple 24 hour reaction steps coupled with separation of the intermediate product via cationic exchange before hydrogel formation by UV radiation. Similarly, another pH sensitive inulin hydrogel was synthesized by reaction with divinyl sulfone and then succinic anhydride, before crosslinking the derivative with a tri-thiolated reagent to form a hydrogel [41]. Again, this process was time consuming (about 56-96 hours), requiring a three step process before formation of the hydrogel as well as cationic exchange for separation of intermediate products. The currently reported methods clearly show the benefit of an alternative synthesis method that circumvents the time consuming, multiple step processes used for the synthesis of pH sensitive inulin hydrogels.

Dianhydrides provide a convenient method to crosslink many materials due to their ready reactivity with nucleophiles, such as the hydroxyl groups on polysaccharides. In particular, there is increasing interest in the use of PMDA as a crosslinker to form

superabsorbent hydrogels with polyvinyl alcohol as well as from modified polysaccharides such as chitosan and cellulose acetate [45-48].

In addition, the formation of colloidal nanoporous materials (nanosponges) by crosslinking cyclodextrins [49] and maltodextrin [50] with pyromellitic anhydride has been reported using one-pot reactions with potential for encapsulating drugs/organic substances for pharmaceutical and biomedical applications. Furthermore, a cyclodextrin based nanosponge with ester linkages has been reported by crosslinking with a polycarboxylic acid using dianhydrides and showed excellent swelling in water (25 fold weight increase) [51].

We hypothesized that the chemical cross-linking between inulin and varying amount of PMDA will produce novel pH sensitive hydrogel with different degree of crosslinking density. The aim of this study is to crosslink inulin with PMDA via esterification reaction to produce pH sensitive hydrogel. To our knowledge, this is the first report that uses PMDA to crosslink inulin in a novel room temperature one pot synthesis through esterification of inulin hydroxyl groups. The smart inulin hydrogels were prepared from inulin according to the procedure outlined in Figure 1 and table 1. This process constructs an inulin hydrogel more conveniently than previous procedures, introducing ionizable carboxylic acid groups in the same step that forms the hydrogel structure, creating a smart platform with potential as carrier for colon targeting delivery.

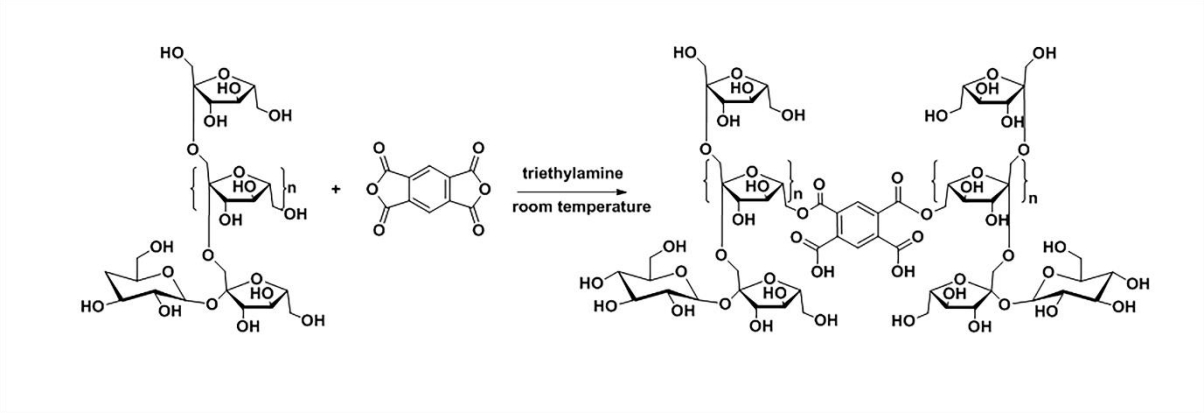

Figure 1- Esterification of inulin with pyromellitic dianhydride

Table 1 showing the different amount of crosslinker in the hydrogel synthesis

Hydrogel	Inulin (g)	PMDA (g)	Inulin OH mmol/PMDA mmol Ratio
IN93HY1	0.5	0.134	15
IN93HY2	0.5	0.268	7.5
IN93HY3	0.5	0.402	5

2. Experimental

2.1 Materials

Inulin from Dahlia Tuber with average chain length (DPn) 39.2 and MWn = 6381.7 as determined by ^{1}H NMR method previously reported by Barclay et al. [52] (Table S1, Figure 1A and 2A from supporting information), PMDA, dimethylformamide (DMF) 99.9 %, triethylamine, hydrochloric acid, diethyl ether, ethyl acetate, hexane, chloroform, phosphate-buffered saline (PBS) tablets were all purchased from Sigma-Aldrich Australia. Sodium hydroxide obtained from Ajax FineChem (Australia), acetone from Merck (Australia) and ethanol from Thermo Fischer (Australia). All chemicals were of analytic grade and used as received. High purity water was obtained from a Sartorius™ Arium pro Ultrapure Water System operating at 18.2 MΩ.

2.2 Hydrogel synthesis

Before synthesis, the raw inulin from Sigma was dried for 24 hours at 70°C to remove any traces of water. Inulin (0.25g, 4.725 mmol OH group) was solubilized in DMF (2 mL) under constant stirring at 400 rpm. Then PMDA (0.6, 1.22 and 1.84 mmol) was dissolved separately in DMF (2 mL) under constant stirring (400 rpm). After complete dissolution of inulin and PMDA, the solutions were mixed with vigorous stirring at 400 rpm for 2 hours before the addition of triethylamine (400µl) resulting in increased viscosity, changing from a solution to a gel in less than 5 minutes. The reaction was continued at room temperature for 24 hours before the hydrogel product was removed from the flask and cut into small pieces of approximately 1 cm^{-3}. The hydrogel was soaked in 20% aqueous ethanol for 5 days

and then washed with high purity water for 10 days, removing the solvent and unreacted reagents. [53, 54] The effectiveness of the washing was confirmed by monitoring the wash liquid for the presence of PMDA by UV absorption.

The final product was dried at 25 °C for 4 days and then stored in a desiccator.

2.3 Determination of the carboxylic acid content

The carboxyl acid content of the inulin hydrogel was determined using acid-base back titration. Each hydrogel batch (100mg) was added to an excess of sodium hydroxide solution (0.1 M, 20 mL) and stirred for 24 hours to allow for complete ester hydrolysis. The excess amount of sodium hydroxide was then titrated against hydrochloric acid (0.1 M) using phenolphthalein as an indicator. The carboxyl content in miliequivalents per 100g of the hydrogel was calculated using the equation below.

$$\%\ \mathrm{COOH\ content} = \frac{\{(\mathrm{Vb} - \mathrm{Va})\ \mathrm{X}\ \mathrm{M}\ \mathrm{X}\ 100\}}{\mathrm{W}} \qquad (1)$$

Where V_b is the volume of hydrochloric acid used for the back titration in the absence of the sample, V_a is the volume of acid used in present of the sample, M is the concentration of the hydrochloric acid and W is the weight of dried hydrogel sample used in the titration. All experiments for the titration were performed in triplicate and average value reported.

2.4 UV spectrophotometry

Hydrogel hydrolysates were analysed for aromatic rings from the crosslinker using a Thermo Evolution 201 UV-VIS spectrophotometer Thermo Fisher Scientific (USA) and scanning wavelengths from 240-310 nm. Pure inulin hydrolysate was used as the background.

2.5 Characterization of the smart hydrogel using Fourier transform infrared spectroscopy (FTIR)

FTIR spectra of inulin, PMDA and inulin hydrogel samples were obtained using a Shimadzu FTIR-8400S Spectroscope (Japan) from freeze-dried material prepared into KBr discs by grinding the sample (2 mg) and KBr (100mg; FTIR grade) to a fine powder. The powder was then compressed into discs using 8 tonnes of pressure. The final disc produced were scanned from 4000 to 400 cm^{-1} using 32 scans with a resolution of 4 cm^{-1}.

2.6 Thermogravimetric analysis (TGA)

Inulin, PMDA and hydrogel were weighed (6 ± 0.1 mg) and TGA analysis was carried out using a Thermogravimetric Analyzer Discovery TGA 550 **(**USA) under a nitrogen flow of 10 mL min^{-1} with a heating rate of 10°C/min between room temperature and 500°C.

2.7 Differential Scanning Calorimetry (DSC)

DSC of the inulin hydrogel and raw inulin sample was carried out using a Discovery DSC TA Instruments (model Discovery DSC 2920 USA) calibrated with an indium standard. Dry samples (2 ± 0.1 mg) were analyzed by heating from room temperature to 250°C at a rate of 10 °C/min under a nitrogen atmosphere (10 mL min^{-1}).

2.8 Scanning electron microscope (SEM)

SEM was conducted using a Zeiss Merlin Field Emission Gun Scanning Electron Microscope (Germany). Prior to the analysis, inulin hydrogels were swollen in distilled water for at least 48 hours before freeze drying. The samples were then placed on double side tape before sputter coating with platinum (approximately 5 nm) and then examined using an accelerating voltage of 2-5 kV.

2.9 Determination of water absorbency and swelling kinetics

The swelling characteristics of the synthesized hydrogels were determined at 37°C in hydrochloric acid (HCl; 0.1 M) as well as citrate (0.1M and pH 4.5) and PBS (pH 7.4, 0.01 M) buffers prepared from high purity water (more detail on buffer preparation in supplementary information) and all measurements were conducted in triplicate and average value reported. The smart hydrogels were taken from the swelling medium at specific intervals and blotted with tissue paper in order to remove surface water and then the swollen hydrogel was weighed. The following equation was used in calculating the swelling ratio (2) and the percentage of swelling (3)

$$\text{The swelling ratio of the hydrogel} = \frac{(Ws - Wd)}{Wd} \quad (2)$$

$$\%S = \frac{(Ws - Wd)\ X\ 100}{Wd} \quad (3)$$

Where W_d represents the dry weight of the hydrogel before swelling W_S is the weight of the hydrogel at different time intervals during the swelling.

2.10 Crosslinking density determination using Flory-Rehner Theory

About (~100mg) of samples from IN93HY1, IN93HY2 and IN93HY3 hydrogel batches (Hydrogel synthesized from 0.6, 1.22 and 1.84 mmol PMDA respectively) were allowed to swell in eight different solvents with different solubility parameters (see Table 1) for 10 days in the dark in order to reach equilibrium. The weight of the swollen hydrogel was determined before and after removing the solvents by vacuum drying. The maximum swelling at equilibrium and percentage swelling was determined using equations (2) and (3) above respectively. The determination of the crosslinking density and average molecular weight between cross-links was obtained from the equilibrium swelling data for the best solvent (water) using Flory-Rehner Theory. The density of the different hydrogels was determined with a pycnometer using hexane as the solvent. All experiments for the density measurement were performed in triplicate and average value reported.

Table 2: Solvents Solubility Parameters [47, 55].

Solvents	Solubility Parameters $(cal/cm^3)^{1/2}$
Ethyl Ether	7.4
Ethyl acetate	9.05
Chloroform	9.3
Acetone	9.9
Ethanol	26.2
Water	23.4
DMF	12.1

In this hydrogel swelling experiment, we assumed affine deformation which enables the calculation of the crosslink density using equation 4 below.[47]

$$\nu = \frac{[\ln(1 - Vr) + Vr + \chi\, Vr^2]}{\rho\, V1\, (Vr^{1/3} - Vr/2)} \qquad (4)$$

Where ν represent the crosslink density of the hydrogel, ρ is density of the hydrogel, χ is the parameter of interaction between the solvent and polymer (see equation 7) and Vr is the polymer volume fraction or reduced volume calculated from equation 5.

$$\mathrm{Vr} = [1 + \rho/\rho s\, (\mathrm{Ms}/\mathrm{Md} - 1)] \qquad (5)$$

Where Ms is the swollen polymer weight, Md is the weight of the dried hydrogel before swelling experiment and ρ_s is the density of the solvent

Average molar mass between crosslink points (Mc) is then calculated from equation 6 below

$$\nu = \rho/\mathrm{Mc} \qquad (6)$$

Based on Flory and Rehner theory, three forces control the swelling of hydrogel and this can be simplified as shown in equation 7 [56]. The controlling forces during swelling are the positive change in entropy caused by the mixing the solvent and polymer, the opposing negative change in the entropy caused by the elasticity of the gel as it swells due to the reduced number of chain conformations possible in a crosslinked network and the enthalpy of mixing of the solvent and polymer[56].

$$\chi = \chi\mathrm{h} + \chi s \qquad (7)$$

Where the forces imposed entropy and enthalpy are represented by χs and χh respectively.

When the hydrogel swells to equilibrium, it is assumed that the contribution of the enthalpy component (χh) is negligible meaning that the parameter of interaction between the solvent and polymer, χ, is equal to the contribution from the χs entropic component only [47]. In this work, the literature value of 0.473 for dextran was used for the Flory polymer-solvent interaction parameter for inulin [57] because currently there is no literature value for inulin. In these swelling experiments, all the hydrogels had maximum swelling in water and so the solubility parameter equal that of water. The maximum swelling in equilibrium which is represented as Q was determined from the equation 8 below

$$Q = \frac{(Ms - Md)}{Md \times \rho} \qquad (8)$$

Where Ms is the swollen hydrogel weight and Md is the weight of the dried hydrogel before swelling experiment.

3. Results and discussion

3.1 Hydrogels synthesis

Preparation of the hydrogel

The preparation of the smart inulin hydrogel proceeded by the esterification of hydroxyl groups from inulin with the PMDA crosslinker using triethylamine as a catalyst (Figure 1)[55]. This process resulted in the formation of a three dimensional polymer network that swells rapidly in water with a small proportion of grafting of monoester species possibly for the highly crosslinked hydrogels. By varying the ratio of the crosslinker used in the reaction, hydrogels of different crosslinking density were obtained (Figure 1) demonstrated by changes in the physical appearance of the hydrogel. Hydrogel synthesised with low amounts of PMDA was milky white while higher amounts revealed a glassy transparent appearance. Preliminary work showed that a PMDA quantity between 0.461 and 2.295 mmol was necessary for the

formation of a hydrogel with 0.25 grams of inulin with the right amount of crosslinking for satisfactory mechanical and swelling properties. This is because hydrogels formed with less than 100mg of PMDA had poor integrity and were easily eroded during washing and too much PMDA resulted in hard, glassy hydrogels with poor swelling.

3.2 Carboxylic acid

Each anhydride ring opening of PMDA in the esterification with inulin results in the formation of one carboxylic acid group in the crosslinker. Consequently, determination of the number of free carboxylic acid groups in the polymer network provides information on the extent of crosslinking in the smart hydrogel. Back titration of hydrolysed hydrogels demonstrated the expected increase in carboxylic acid content with increased PMDA in the crosslinking reaction from 0.134g to 0.402g (see Table 3). The ionic carboxylate pendant groups confer the hydrogel with pH sensitive properties that can be tuned and utilized as a trigger for its swelling and release of encapsulated drugs from the hydrogel.

Table 3 showing the Total carboxylic acid content (mEq/100 g) of the hydrogels

Hydrogel	Hydrogel amount (mg)	Vb –Va(mL)	Total carboxylic acid content (mEq/100 g)
IN93HY1	100	3.2	315.2
IN93HY2	100	4.8	472.8
IN93HY3	100	7.2	709.2

3.3 UV spectrophotometry

The UV spectra of the hydrogels after alkaline hydrolysis with sodium hydroxide shows an increase in the absorption maxima at ~ 295 nm attributed to π-π∗ transitions of PMDA aromatic group moiety in the crosslinking agent [45, 58]. This result clearly demonstrates that crosslink density increases with increasing PMDA in the crosslinking reaction (Figure 2) [45]. This finding is also consistent with the visual assessment of the hydrogel and back titration results.

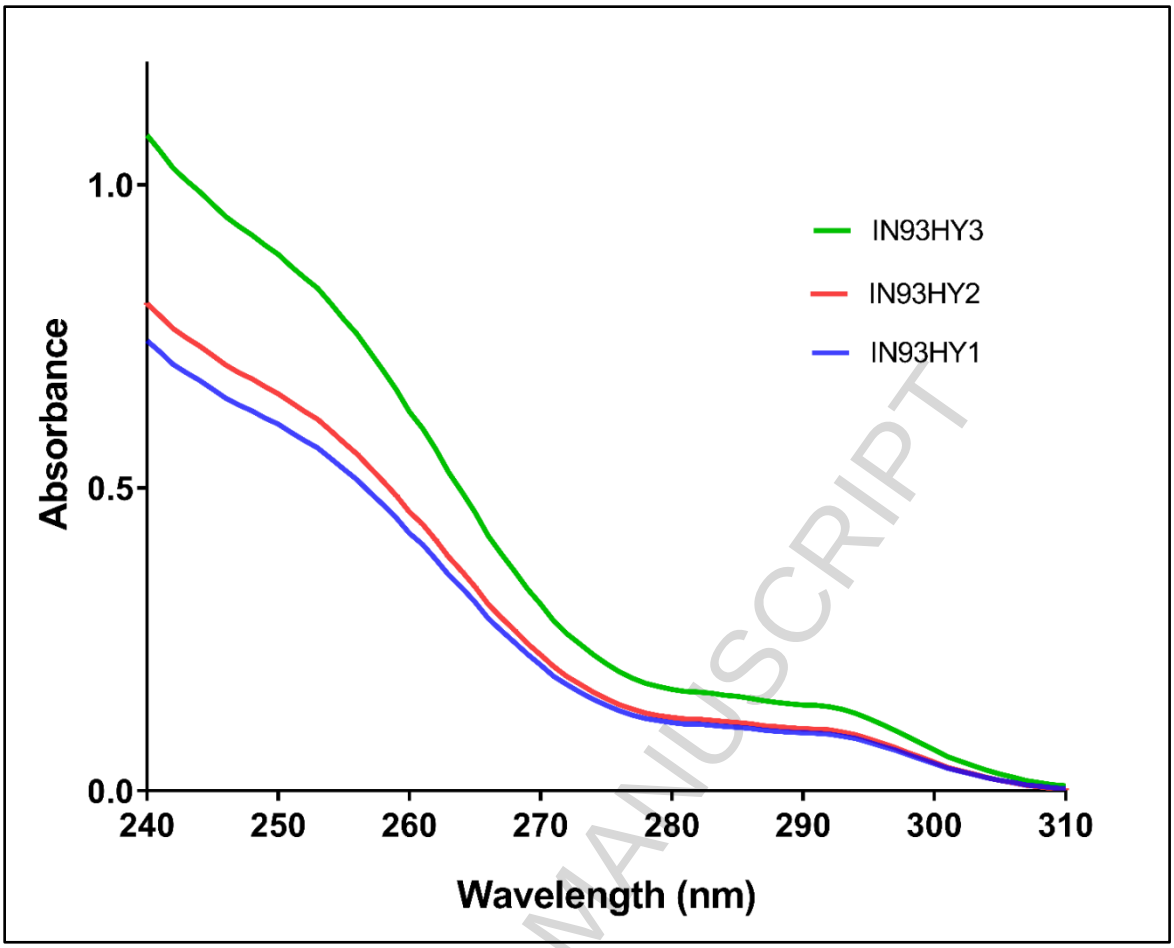

Figure 2: UV spectrum of Inulin-PMDA hydrogel after alkaline hydrolysis

3.4 FTIR Analysis

FTIR was used to confirm the formation of new biomaterial from the crosslinking of inulin with PMDA. The pure inulin is characterized by bands at 3363 cm^{-1}, 2926 cm^{-1}, 1028 cm^{-1} that are assigned to OH stretching, aliphatic CH_2 stretching and COC bending respectively.[10] Other important bands include those at 1170 cm^{-1}, 934 cm^{-1}, 873 cm^{-1}, and 817 cm^{-1} and two shoulders at 1132 cm^{-1} and 986 cm^{-1} (Figure A1 supporting data) [10] The hydrogel has new absorption bands in the FTIR spectrum attributed to carbonyl groups (**C=O)** at 1729 cm^{-1} and 1395 cm^{-1} and to the ester linkages at 1592 cm^{-1}. There is also a new band at 713 cm^{-1}, attributed to the aromatic ring out of plane angular vibration from the C-H bond of the pyromellitic group.

The hydrogel has new absorption bands in the FTIR spectrum attributed to carbonyl groups at 1729 cm^{-1} and 1395 cm^{-1} from the ester linkages and at 1592 cm^{-1} due to

the carboxylic acid moieties (Figure 3A and 3B) [47, 59]. There is also a new peak at 713 cm^{-1}, attributed to the aromatic ring out of plane angular vibration from the C-H bond of the pyromellitic group.

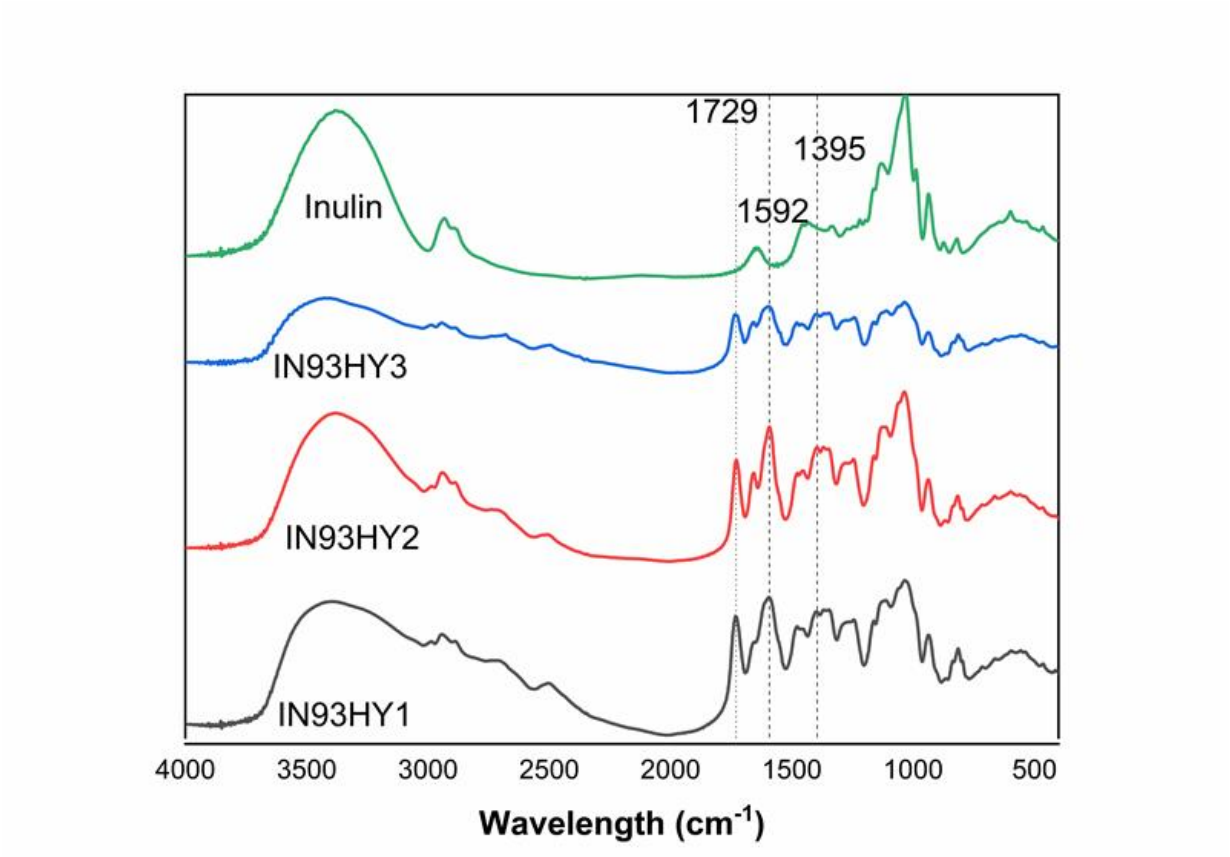

Figure 3A showing FTIR spectra of inulin and all the hydrogel from 4000 to 400 cm^{-1}

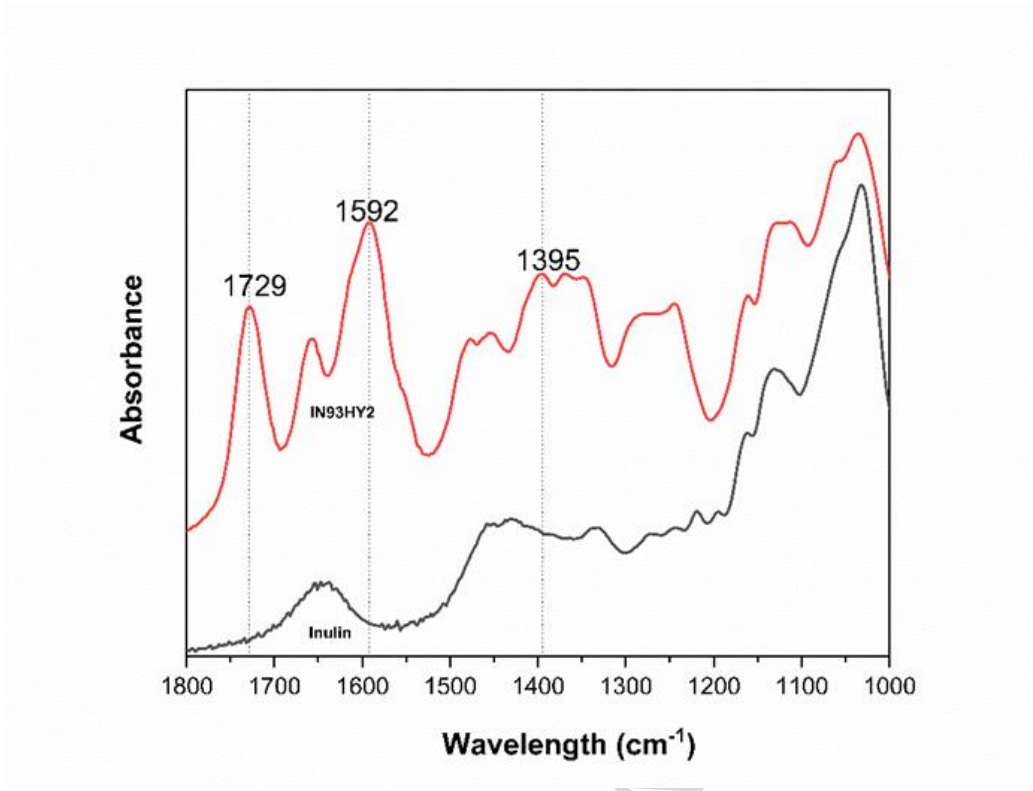

Figure 3B showing FTIR spectra of both inulin and IN93HY2 from 1800 to 1000 cm^{-1}

3.5 TGA

TGA analysis was used to assess the thermal stability of the raw inulin and hydrogel samples. The TGA results show that the hydrogels have lower thermal stability when compared to inulin due to the formation of the relatively thermally unstable ester linkage formed during crosslinking reaction, as previously noted in the literature for related ester products [47, 60-62]. The TGA thermograms of the starting materials are in Figure 4 which shows that PMDA thermally degrades between 271°C and 283°C. The thermogram of pure inulin in Figure 4 shows the major weight loss of ~ 55% occurs due to the degradation of the inulin backbone in the temperature range of 225°C to about 320°C and is consistent with the result obtained by Dan et al [63]. TGA of the smart inulin hydrogels shows that all hydrogel have similar thermal degradation behaviour that contrasts to raw inulin, with three stages of weight loss events. The first stage was due to the loss of water content and volatile materials in the hydrogel [47] followed by degradation of ester crosslinks and the third stage is mainly attributed to the degradation of the inulin chains (Figures 4).The first stage

thermal event results in weight loss of about 6.35, 5.88 and 5.67% for hydrogel IN93HY1, IN93HY2 and IN93HY3 respectively. The thermograms of the hydrogels also result in greater residual weight than inulin (between 30.5 to 31.5%) after the TGA analysis possibly due to the increased carbon - carbon network, thermo-oxidative stability and heat resistant properties of the crosslinker [64]. The thermal degradation properties of the hydrogels provides physical confirmation of the chemical analysis of the inulin derivative formed by the crosslinking of the inulin chains by PMDA. Despite the reduction in the thermal stability of the hydrogel compared to inulin, it is clear that the hydrogel samples are quite stable and its stability will not be affected at the physiological temperature (37).

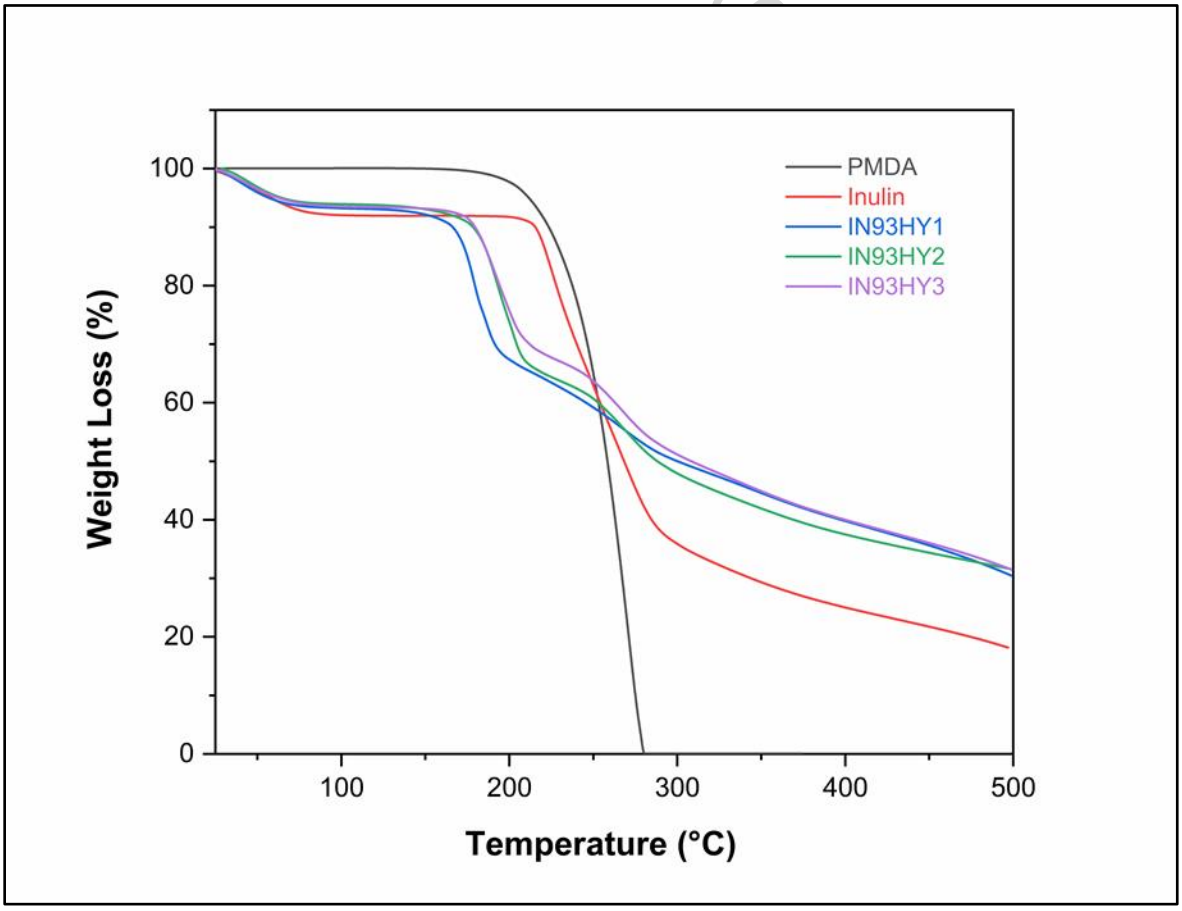

Figure 4 TGA thermograms of raw inulin, PMDA and hydrogels IN93HY1, IN93HY2 and IN93HY3

3.6 DSC

The DSC of the pure inulin sample shows endothermic transitions occurring between ~ 167 ºC and 185 ºC due to melting of various semicrystalline isoforms [65, 66] with possibly a glass transition occurring concurrently with initial melting at 167ºC [65] before the degradation at 226 ^{o}C (Figure 5). Contrasting to the unmodified inulin, the hydrogel DSC is characterized by endothermic peaks between 179,184 and 186 ºC for INU93HY2, INU93HY1 And INU93HY3 respectively that are due to the degradation of the ester bond followed by broad exothermic transitions for all the hydrogels due to reactions such as dehydration and formation of anhydrides from the carboxylic acid groups and inulin OH group in the hydrogel [67]. This is consistent with results obtained from other polysaccharides and modified polysaccharides such as hyaluronic acid [67] and cellulose acetate [68].

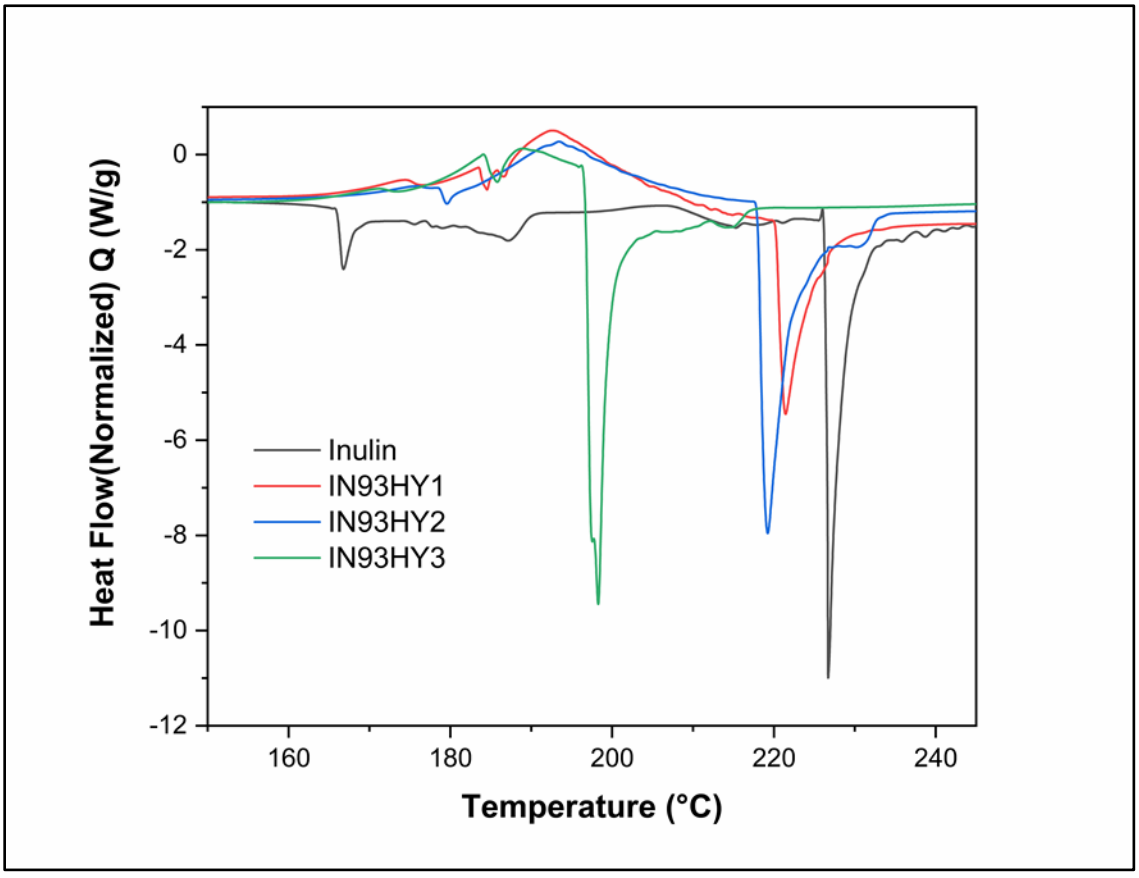

Figure 5 DSC thermograms of unmodified inulin and the different hydrogel batches.

3.7 Scanning electron microscope (SEM)

The SEM from Figure 6A-D clearly shows changes in the surface morphology of inulin after crosslinking with PMDA. Pure inulin appears as spherical smooth aggregates [63, 69] typical of spray dried powders. (Figure 6A) In sharp contrast, the crosslinked material is comprised of more irregular flakes of material (Figure 6B-D) that appear to have folded ridges. The fractures in the material also seem to suggest that the hydrogel is rigid and brittle when dried. This result is in accordance with the literature, which reports that crosslinking polymers with PMDA result in the formation of irregular sponge like materials. [45, 70]

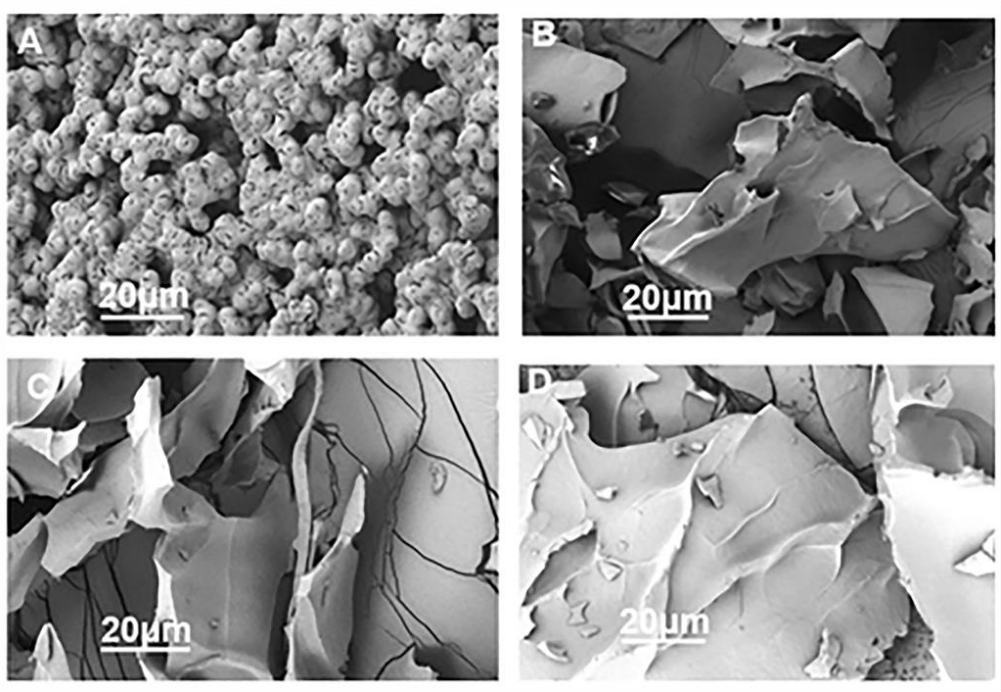

Figure 6 SEM images of raw inulin (A) and the different hydrogels IN93HY1 (B), IN93HY2(C) and IN93HY3 (D)

3.8 Swelling

Swelling experiments were performed in water and buffers at 37°C. Figure 7A shows a rapid increase in swelling ratio for the first 6 hours of immersion in water, followed

by plateauing of the swelling ratio up to 24 hours for all three hydrogels. Consequently, 24 hours of immersion was taken as the equilibrium swelling time for subsequent measurements. For comparison, hydrogels obtained from PMDA crosslinking exhibited high swelling capacity in water than previously reported pH responsive inulin hydrogel. The swelling ratio of INU-PMDA in water was greater, around 19.2 compared with 3.5 and 6.5 for other pH sensitive inulin hydrogel. [34, 71] Figure 8 also shows that increasing crosslink density results in reduced swelling and this behaviour was consistent in the swelling experiments performed in buffers (Figure 7B) and makes sense as higher crosslink density restricts the swelling of hydrogel due to more compact hydrogel structure [72, 73]. In the buffers, each of the hydrogels had a significant increase in swelling with increasing pH from 1.2 to 7.4. At low pH, less swelling is observed due to the presence of protonated carboxylic acid groups and as the pH increases the carboxylic acid groups are deprotonated and swelling increases [59].

This behaviour is attributed to deprotonation both increasing electrostatic repulsions [34] between these groups, opening up more space in the structure, and increasing the osmotic pressure of the hydrogel, driving water into the structure [59, 74] Similar behaviour has been reported for pH sensitive inulin hydrogels prepared with pendant carboxylic acids groups by modification with acrylic acid [59] and succinic anhydride [34]. This property enables targeted release of drugs encapsulated into hydrogel as reduced swelling in the acidic environment of the stomach allows the hydrogel to protect the encapsulated drug from degradation and prevent premature release in the stomach. Release is then promoted by increased swelling at neutral pH in the colon, encouraging further testing for the potential use of this hydrogel in colon targeted drug delivery.

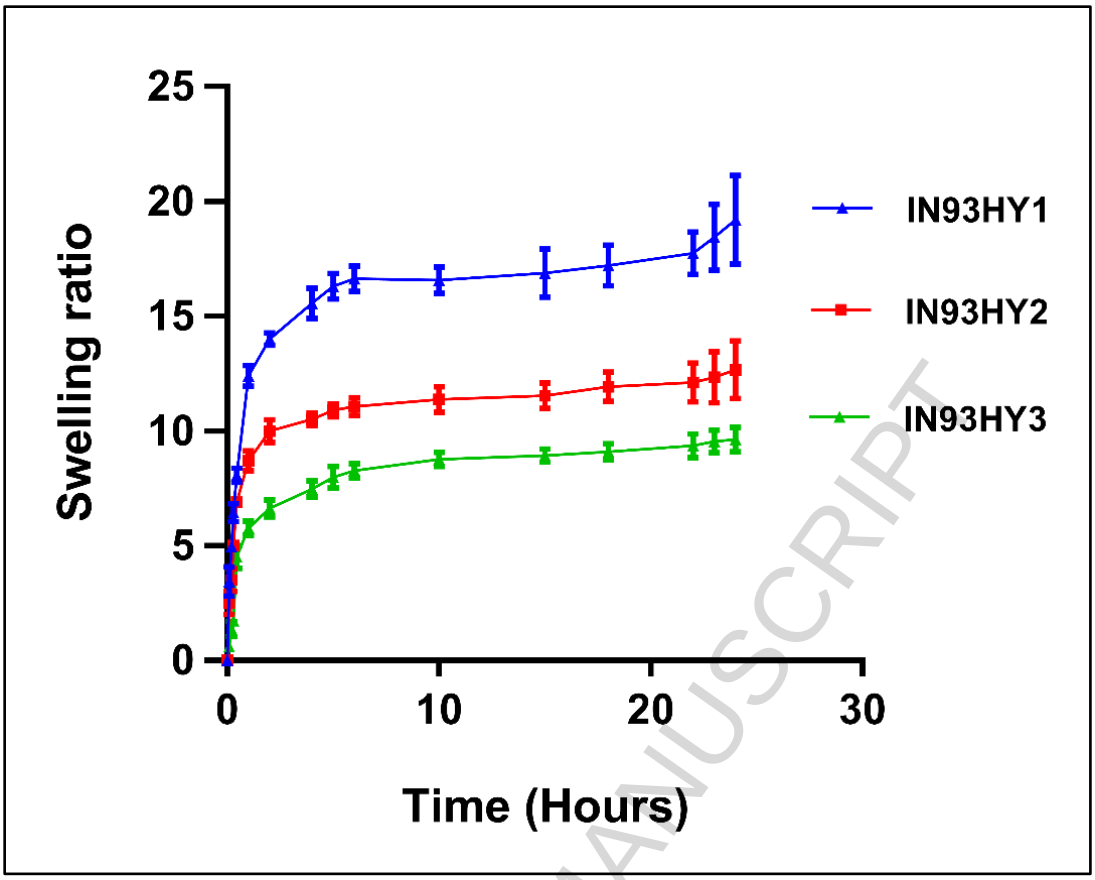

Fig. 7A Hydrogel swelling in de-ionized water

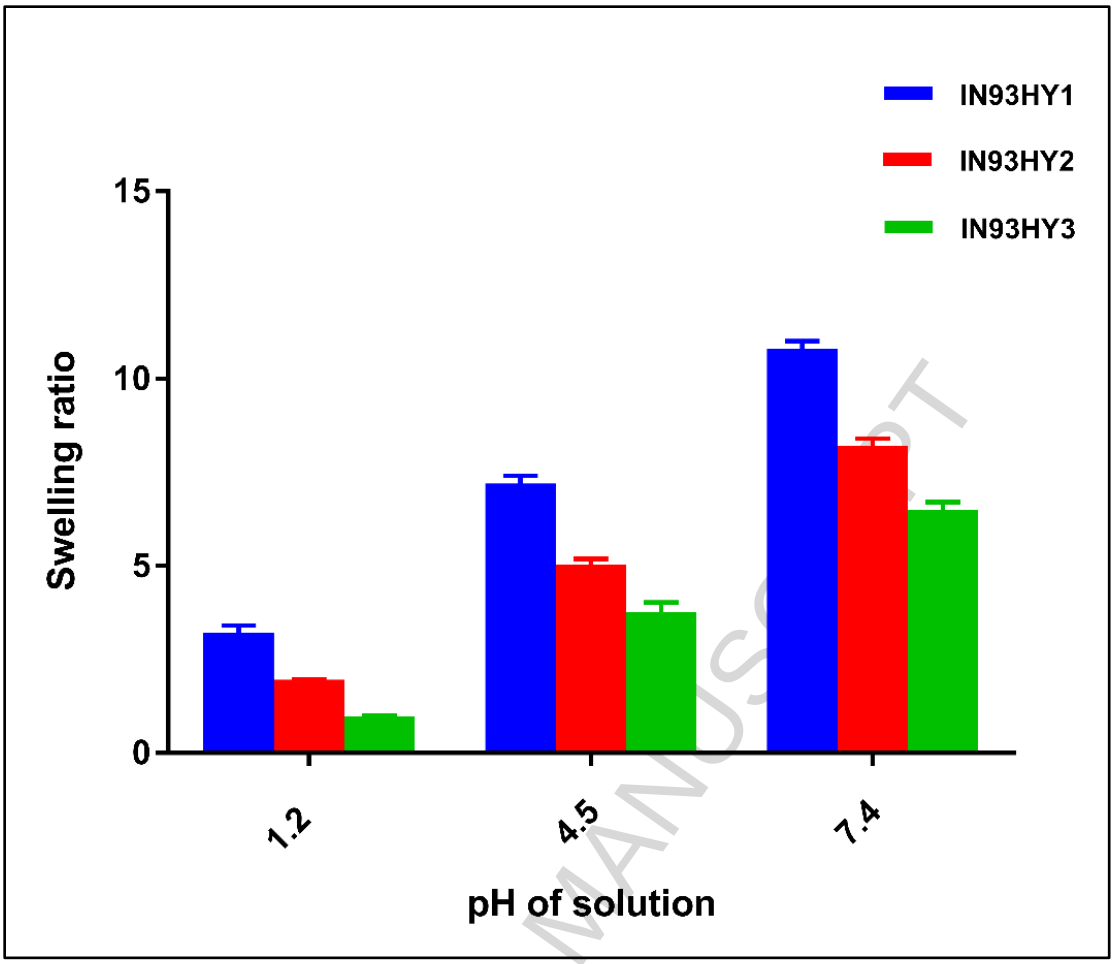

Fig. 7 (B) Swelling ratio in HCl (0.1N, pH 1.2), citrate buffer (pH 4.5), PBS (pH 7.4)

3.9 Crosslinking density determination

Characterization of the parameters of the hydrogel network, such as crosslink density and average molecular weight between cross-links, is important as these aspects determine the amount of solvent that the hydrogel can absorb. In the initial swelling experiment, seven different solvents were tested and all the smart hydrogels had the best swelling in water. This result indicates the polymeric network formed during the crosslinking of inulin and PMDA is dominated by hydrophilic character due to the carboxylic acid pendant groups and inulin's hydroxyl groups despite the hydrophobicity of the PMDA aromatic group. Hydrogel IN93HY1 gels show 1540 % swelling in water at 25 $^{\circ}$C when compared to its dry mass and this excellent water absorption means the hydrogel is defined as superabsorbent (swelling percentage of the hydrogels in the different solvents is reported in Table A2 of the supplementary information). As the concentration of PMDA increased in the crosslinking reaction,

the swelling capacity of the hydrogels formed was diminished as was the average molecular weight between cross-links and the crosslinking density increases (Table 4). This is in agreement with the back titration and UV chemical analyses and makes sense as the increased incorporation of PMDA crosslinker in the hydrogel reduces the space between crosslinks on the inulin chains, increases the number of connections between inulin chains and reduces the space for solvent accommodation, which ultimately results in less swelling.

Table 4 Structural characterization of the hydrogel using Flory-Rehner theory

Hydrogel	**IN93HY1**	**IN93HY2**	**IN93HY3**
Percentage of absorption in the equilibrium (% S)	1540	648	502
Maximum swelling in the equilibrium QMax (cm^3/g)	15.4	6.48	5.02
Reduced Volume Vr	0.045	0.088	0.109
Density of the gel ρ2(g/cm^3)	1.498	1.59	1.6153
Solubility parameter of the hydrogel,δ_2	23.4	23.4	23.4
Interaction parameter polymer-solvent	0.473	0.473	0.473
Density Crosslink, (g/cm^3)	3.84×10^{-3}	8.07×10^{-3}	1.06×10^{-2}
Average Molar Mass between crosslink points (Mc)	390.6	197.03	152.39

4. Conclusion

A novel, smart inulin hydrogel with carboxylic acid pendant groups at each cross-linking site was synthesized via esterification of inulin with PMDA at room temperature in a simple one pot synthesis. Physicochemical characterization of the new polymeric material was performed using techniques such as back titration, FTIR, TGA, DSC, UV, SEM and swelling experiments. By varying the ratio of PMDA, hydrogels with different crosslinking density can be obtained. Importantly, the high swelling in water is pH dependent and supports further investigation of this hydrogel as a potential carrier for colon targeting delivery in which the swelling and mechanical properties can be balanced for optimised drug release.

Acknowledgments

The authors would like to thank Arafat Mohammad and Paris Fatemeh Fouladian for help with SEM, Karen Teague for assistance with laboratory set-up, Dr. Anton Blencowe and Paula FacalMarina for help with hydrogel characterization. This research work was also supported by a grant from the Australian Research Council's Linkage Projects funding scheme (Project number LP140100142).

Appendix A: Supporting data or supplementary data attached to this article

Data availability' section

The raw data required to reproduce these findings are available to download from the Supplementary data

References

1. Kaur, N. and A.K. Gupta, *Applications of inulin and oligofructose in health and nutrition.* J Biosci, 2002. **27**(7): p. 703-14.
2. Mensink, M.A., et al., *Inulin, a flexible oligosaccharide I: Review of its physicochemical characteristics.* Carbohydr Polym, 2015. **130**: p. 405-19.
3. Barclay, T., et al., *Inulin - A versatile polysaccharide with multiple pharmaceutical and food chemical uses.* Journal of Excipients and Food Chemicals, 2010. **1**(3): p. 27-50.
4. Grasmeijer, N., et al., *Unraveling protein stabilization mechanisms: Vitrification and water replacement in a glass transition temperature controlled system.* Biochimica et Biophysica Acta (BBA) - Proteins and Proteomics, 2013. **1834**(4): p. 763-769.
5. Haj-Ahmad, R.R., et al., *Compare and contrast the effects of surfactants (Pluronic®F-127 and Cremophor®EL) and sugars (β-cyclodextrin and inulin) on properties of spray dried and crystallised lysozyme.* European Journal of Pharmaceutical Sciences, 2013. **49**(4): p. 519-534.
6. Saluja, V., et al., *A comparison between spray drying and spray freeze drying to produce an influenza subunit vaccine powder for inhalation.* Journal of Controlled Release, 2010. **144**(2): p. 127-133.
7. Hinrichs, W.L., M.G. Prinsen, and H.W. Frijlink, *Inulin glasses for the stabilization of therapeutic proteins.* Int J Pharm, 2001. **215**(1-2): p. 163-74.
8. Wahjudi, M., et al., *Development of a dry, stable and inhalable acyl–homoserine–lactone–acylase powder formulation for the treatment of pulmonary Pseudomonas aeruginosa infections.* European Journal of Pharmaceutical Sciences, 2013. **48**(4–5): p. 637-643.

9. Srinarong, P., et al., *Strongly enhanced dissolution rate of fenofibrate solid dispersion tablets by incorporation of superdisintegrants.* European Journal of Pharmaceutics and Biopharmaceutics, 2009. **73**(1): p. 154-161.
10. Fares, M.M., M.S. Salem, and M. Khanfar, *Inulin and poly(acrylic acid) grafted inulin for dissolution enhancement and preliminary controlled release of poorly water-soluble Irbesartan drug.* Int J Pharm, 2011. **410**(1-2): p. 206-11.
11. Silva, D.G., P.D. Cooper, and N. Petrovsky, *Inulin-derived adjuvants efficiently promote both Th1 and Th2 immune responses.* Immunol Cell Biol, 2004. **82**(6): p. 611-6.
12. Cooper, P.D. and E.J. Steele, *The adjuvanticity of gamma inulin.* Immunol Cell Biol, 1988. **66 (Pt 5-6)**: p. 345-52.
13. Korbelik, M. and P.D. Cooper, *Potentiation of photodynamic therapy of cancer by complement: the effect of γ-inulin.* British Journal of Cancer, 2007. **96**(1): p. 67-72.
14. Cooper, P.D. and M. Carter, *The anti-melanoma activity of inulin in mice.* Molecular Immunology, 1986. **23**(8): p. 903-908.
15. Cooper, P.D. and M. Carter, *The anti-melanoma activity of inulin in mice.* Mol Immunol, 1986. **23**(8): p. 903-8.
16. Traynor, J., et al., *How to measure renal function in clinical practice.* BMJ : British Medical Journal, 2006. **333**(7571): p. 733-737.
17. Orlando, R., et al., *Determination of inulin clearance by bolus intravenous injection in healthy subjects and ascitic patients: equivalence of systemic and renal clearances as glomerular filtration markers.* British Journal of Clinical Pharmacology, 1998. **46**(6): p. 605-609.
18. Davidson, M.H. and K.C. Maki, *Effects of Dietary Inulin on Serum Lipids.* The Journal of Nutrition, 1999. **129**(7): p. 1474S-1477s.
19. Pourghassem Gargari, B., et al., *Effects of High Performance Inulin Supplementation on Glycemic Control and Antioxidant Status in Women with Type 2 Diabetes.* Diabetes & Metabolism Journal, 2013. **37**(2): p. 140-148.
20. Den Hond, E., B. Geypens, and Y. Ghoos, *Effect of high performance chicory inulin on constipation.* Nutrition Research, 2000. **20**(5): p. 731-736.
21. Marteau, P., et al., *Effects of chicory inulin in constipated elderly people: a double-blind controlled trial.* Int J Food Sci Nutr, 2011. **62**(2): p. 164-70.
22. Leenen, C.H. and L.A. Dieleman, *Inulin and oligofructose in chronic inflammatory bowel disease.* J Nutr, 2007. **137**(11 Suppl): p. 2572s-2575s.
23. Poulain, N., et al., *Microspheres based on inulin for the controlled release of serine protease inhibitors: preparation, characterization and in vitro release.* Journal of Controlled Release, 2003. **92**(1–2): p. 27-38.
24. Lopez-Molina, D., et al., *Cinnamate of inulin as a vehicle for delivery of colonic drugs.* Int J Pharm, 2015. **479**(1): p. 96-102.
25. Vervoort, L., et al., *Inulin hydrogels as carriers for colonic drug targeting: I. Synthesis and characterization of methacrylated inulin and hydrogen formation.* Pharmaceutical Research, 1997. **14**(12): p. 1730-1737.
26. Van den Mooter, G., L. Vervoort, and R. Kinget, *Characterization of methacrylated inulin hydrogels designed for colon targeting: in vitro release of BSA.* Pharm Res, 2003. **20**(2): p. 303-7.
27. Zijlstra, G.S., et al., *Formulation and process development of (recombinant human) deoxyribonuclease I as a powder for inhalation.* Pharmaceutical Development and Technology, 2009. **14**(4): p. 358-368.
28. Sharpe, L.A., et al., *Therapeutic applications of hydrogels in oral drug delivery.* Expert opinion on drug delivery, 2014. **11**(6): p. 901-915.
29. Peppas, N.A., et al., *Hydrogels in pharmaceutical formulations.* Eur J Pharm Biopharm, 2000. **50**(1): p. 27-46.

30. Caló, E. and V.V. Khutoryanskiy, *Biomedical applications of hydrogels: A review of patents and commercial products.* European Polymer Journal, 2015. **65**: p. 252-267.
31. Buwalda, S.J., et al., *Hydrogels in a historical perspective: from simple networks to smart materials.* J Control Release, 2014. **190**: p. 254-73.
32. Van den Mooter, G., L. Vervoort, and R. Kinget, *Characterization of Methacrylated Inulin Hydrogels Designed for Colon Targeting: In Vitro Release of BSA.* Pharmaceutical Research, 2003. **20**(2): p. 303-307.
33. Tripodo, G., et al., *Controlled release of IgG by novel UV induced polysaccharide/poly(amino acid) hydrogels.* Macromol Biosci, 2009. **9**(4): p. 393-401.
34. Castelli, F., et al., *Differential scanning calorimetry study on drug release from an inulin-based hydrogel and its interaction with a biomembrane model: pH and loading effect.* Eur J Pharm Sci, 2008. **35**(1-2): p. 76-85.
35. Pitarresi, G., et al., *Rheological characterization and release properties of inulin-based hydrogels.* Carbohydrate Polymers, 2012. **88**(3): p. 1033-1040.
36. Maris, B., et al., *Synthesis and characterisation of inulin-azo hydrogels designed for colon targeting.* Int J Pharm, 2001. **213**(1-2): p. 143-52.
37. Stubbe, B., et al., *The in vitro evaluation of 'azo containing polysaccharide gels' for colon delivery.* J Control Release, 2001. **75**(1-2): p. 103-14.
38. Sahiner, N., et al., *Synthesis and Properties of Inulin Based Microgels.* Colloids and Interface Science Communications, 2014. **2**(Supplement C): p. 15-18.
39. Mandracchia, D., et al., *New Biodegradable Hydrogels Based on Inulin and alpha,beta-Polyaspartylhydrazide Designed for Colonic Drug Delivery: In Vitro Release of Glutathione and Oxytocin.* J Biomater Sci Polym Ed, 2011. **22**(1-3): p. 313-28.
40. Tripodo, G., et al., *UV-photocrosslinking of inulin derivatives to produce hydrogels for drug delivery application.* Macromol Biosci, 2005. **5**(11): p. 1074-84.
41. Pitarresi, G., et al., *Hydrogels for potential colon drug release by thiol-ene conjugate addition of a new inulin derivative.* Macromol Biosci, 2008. **8**(10): p. 891-902.
42. Pitarresi, G., et al., *Inulin-based hydrogel for oral delivery of flutamide: preparation, characterization, and in vivo release studies.* Macromol Biosci, 2012. **12**(6): p. 770-8.
43. Flamm, G., et al., *Inulin and oligofructose as dietary fiber: a review of the evidence.* Crit Rev Food Sci Nutr, 2001. **41**(5): p. 353-62.
44. Roberfroid, M.B. and N.M. Delzenne, *Dietary fructans.* Annu Rev Nutr, 1998. **18**: p. 117-43.
45. Oliveira, V.A., et al., *Hydrogels of cellulose acetate crosslinked with pyromellitic dianhydride: part I: synthesis and swelling kinetics.* Química Nova, 2013. **36**: p. 102-106.
46. Kavianinia, I., et al., *New hydrogels based on symmetrical aromatic anhydrides: Synthesis, characterization and metal ion adsorption evaluation.* Carbohydrate Polymers, 2012. **87**(1): p. 881-893.
47. Senna, A.M., K.M. Novack, and V.R. Botaro, *Synthesis and characterization of hydrogels from cellulose acetate by esterification crosslinking with EDTA dianhydride.* Carbohydrate Polymers, 2014. **114**: p. 260-268.
48. Yamada, T., M. Karikomi, and T. Kimura, *Preparation of pH-Responsive Polyvinyl Alcohol Hydrogels and Their Drug-Releasing Behavior*. Vol. 69. 2012. 539-542.
49. Swaminathan, S., R. Cavalli, and F. Trotta, *Cyclodextrin-based nanosponges: a versatile platform for cancer nanotherapeutics development.* Wiley Interdiscip Rev Nanomed Nanobiotechnol, 2016. **8**(4): p. 579-601.
50. Trotta F and Fossati E, *U.S. Patent No. 20170130052 A1.* 2017(Washington, DC: U.S. Patent and Trademark Office).
51. Caldera, F., et al., *Evolution of Cyclodextrin Nanosponges*. Vol. 531. 2017.
52. Barclay, T., et al., *Analysis of the hydrolysis of inulin using real time (1)H NMR spectroscopy.* Carbohydrate Research, 2012. **352**: p. 117-125.

53. Senna, A.M., et al., *Synthesis, characterization and application of hydrogel derived from cellulose acetate as a substrate for slow-release NPK fertilizer and water retention in soil.* Journal of Environmental Chemical Engineering, 2015. **3**(2): p. 996-1002.
54. Ruiz, J., A. Mantecón, and V. Cádiz, *Synthesis and properties of hydrogels from poly (vinyl alcohol) and ethylenediaminetetraacetic dianhydride.* Polymer, 2001. **42**(15): p. 6347-6354.
55. Senna, A.M., A.J.d. Menezes, and V.R. Botaro, , *Study of the density of crosslinks in superabsorbent gels obtained from cellulose acetate. .* Polymers,, 2013. **23**:: p. p. 59-64.
56. Flory, P.J. and J. Rehner, *Statistical Mechanics of Cross-Linked Polymer Networks I. Rubberlike Elasticity.* The Journal of Chemical Physics, 1943. **11**(11): p. 512-520.
57. Ferreira, L., et al., *Enzymatic synthesis of inulin-containing hydrogels.* Biomacromolecules, 2002. **3**(2): p. 333-41.
58. Zhang, F. and M.P. Srinivasan, *Ultra thin films of oligoimide through molecular assembly.* Colloids and Surfaces A: Physicochemical and Engineering Aspects, 2005. **257-258**: p. 295-299.
59. Chiu, H.C., Y.H. Hsu, and P.J. Lin, *Synthesis of pH-sensitive inulin hydrogels and characterization of their swelling properties.* Journal of Biomedical Materials Research, 2002. **61**(1): p. 146-152.
60. Botaro, V.R. and P.A. Dantas, *Synthesis and characterization of a new cellulose acetate-propionate gel: Crosslinking density determination*. Vol. 2. 2012. 144-151.
61. Botaro, V.R., C.G. Santos, and V.A. Oliveira, *Hidrogéis superabsorventes a base de acetato de celulose modificado por dianidrido 3,3', 4,4' benzofenona tetracarboxílico (BTDA): síntese, caracterização e estudos físico-químicos de absorção.* Polímeros, 2009. **19**: p. 278-284.
62. Ghorpade, V.S., A.V. Yadav, and R.J. Dias, *Citric acid crosslinked beta-cyclodextrin/carboxymethylcellulose hydrogel films for controlled delivery of poorly soluble drugs.* Carbohydr Polym, 2017. **164**: p. 339-348.
63. Dan, A., S. Ghosh, and S.P. Moulik, *Physicochemical studies on the biopolymer inulin: a critical evaluation of its self-aggregation, aggregate-morphology, interaction with water, and thermal stability.* Biopolymers, 2009. **91**(9): p. 687-99.
64. Abbasi, F., S. Mehdipour-Ataei, and S. Khademinejad, *Novel type of highly soluble and thermally stable poly(sulfone ether imide)s.* Designed Monomers and Polymers, 2015. **18**(8): p. 789-798.
65. Cooper, P.D., et al., *The polysaccharide inulin is characterized by an extensive series of periodic isoforms with varying biological actions.* Glycobiology, 2013. **23**(10): p. 1164-1174.
66. Ronkart, S.N., *Impact of the crystallisation pathway of inulin on its mono-hydrate to hemi-hydrate thermal transition.* Food Chem., 2010. **119**: p. 317-322.
67. Larrañeta, E., et al., *Synthesis and characterization of hyaluronic acid hydrogels crosslinked using a solvent-free process for potential biomedical applications.* Carbohydrate Polymers, 2018. **181**: p. 1194-1205.
68. Botaro, V., C. G. Santos, and V. A. Oliveira, *Synthesis of Hydrogels of Cellulose Acetate (AC) Cross-Linked With 3,3 ',4,4 ' Benzophenonetetracarboxylic Dianhydride (BTDA): Characterization and Adsorption Physicochemical Study*. Vol. 19. 2008. 278-284.
69. Toneli, J., et al., *Spray-Drying Process Optimization of Chicory Root Inulin.* Drying Technology, 2010. **28**(3): p. 369-379.
70. Singh, V., *Ordered and disordered cyclodextrin nanosponges with diverse physicochemical properties*. Vol. 7. 2017.
71. Pitarresi, G., et al., *Hydrogels for Potential Colon Drug Release by Thiol-ene Conjugate Addition of a New Inulin Derivative.* Macromolecular Bioscience, 2008. **8**(10): p. 891-902.
72. Khan, S. and N. Mohammad Ranjha, *Effect of degree of cross-linking on swelling and on drug release of low viscous chitosan/poly(vinyl alcohol) hydrogels*. Vol. 71. 2014. 2133-2158.
73. Yacob, N. and K. Hashim, *Morphological Effect on Swelling Behaviour of Hydrogel*. Vol. 1584. 2014.

74. De, S.K., et al., *Equilibrium swelling and kinetics of pH-responsive hydrogels: models, experiments, and simulations.* Journal of Microelectromechanical Systems, 2002. **11**(5): p. 544-555.

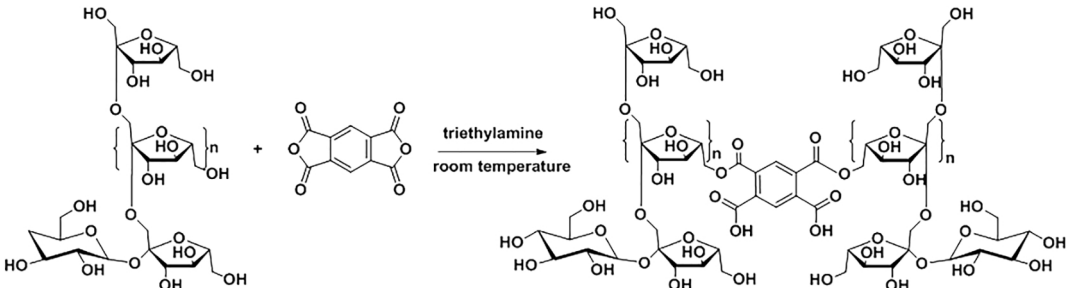

Figure 1

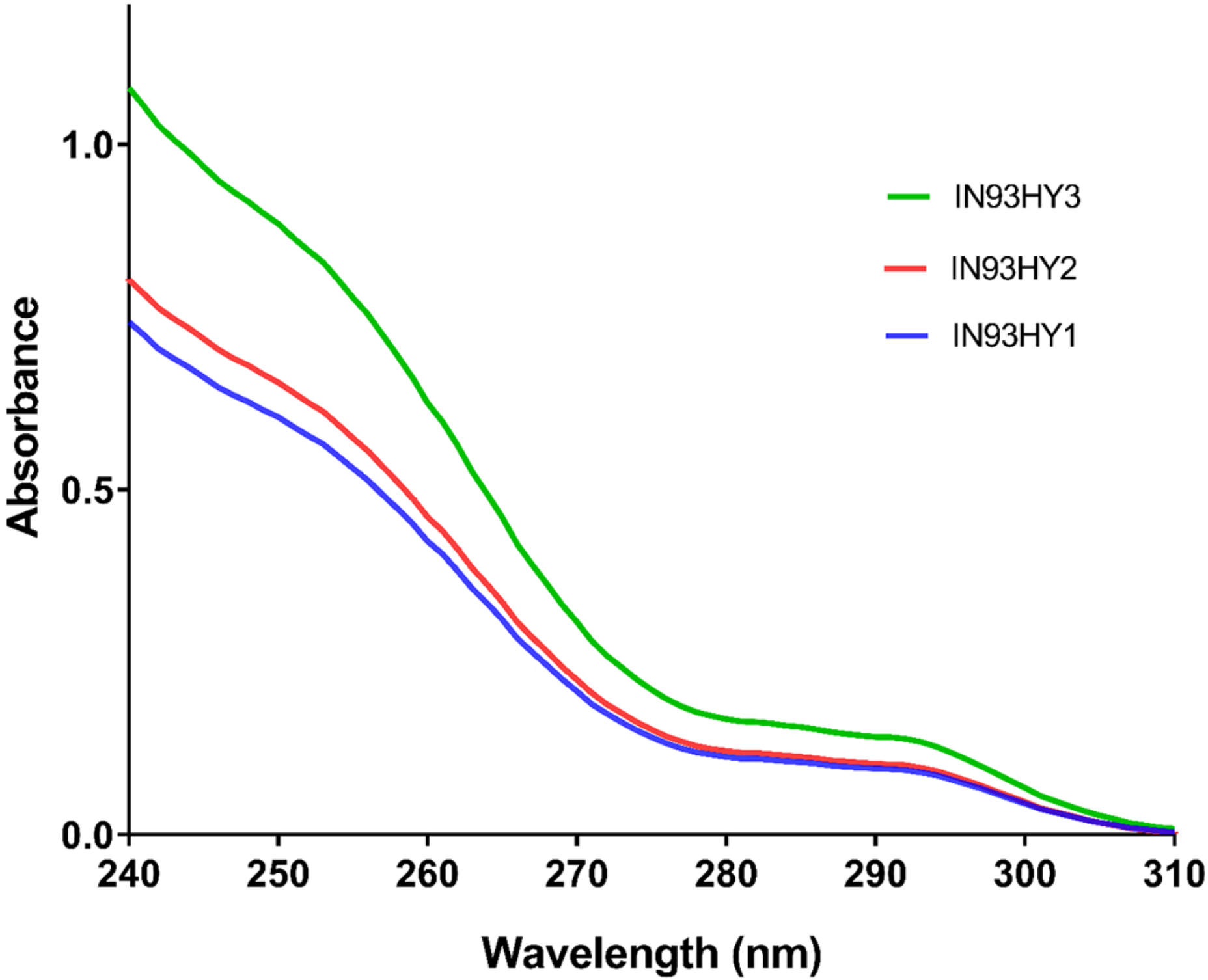
IN93HY3
IN93HY2
IN93HY1
Absorbance
1.0
0.5
0.0
240
250
260
270
280
290
300
310
Wavelength (nm)

Figure 2

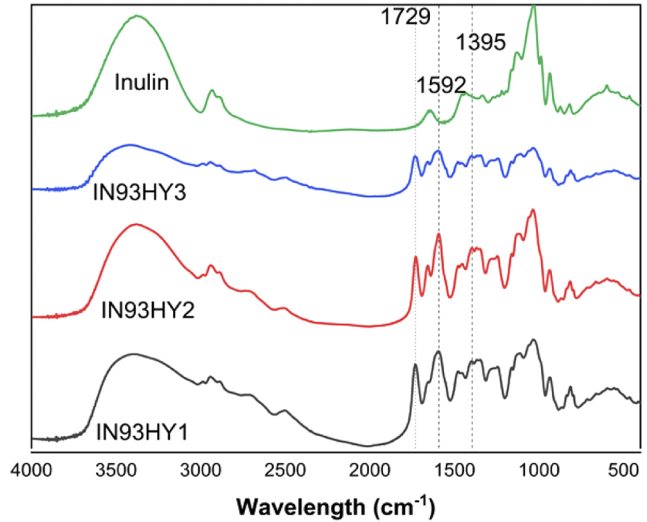
1729
1395
1592
Inulin
IN93HY3
IN93HY2
IN93HY1
4000
3500
3000
2500
2000
1500
1000
500
Wavelength (cm-1)

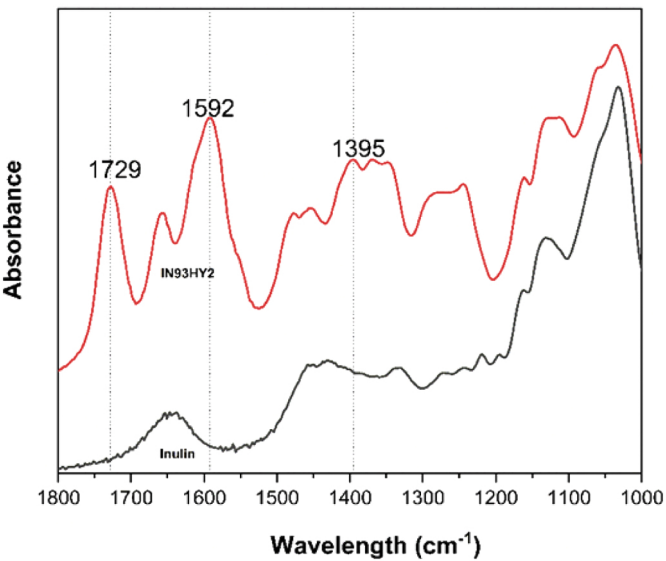
1592
1729
1395
IN93HY2
Inulin
Absorbance
1800
1700
1600
1500
1400
1300
1200
1100
1000
Wavelength (cm-1)

Figure 3

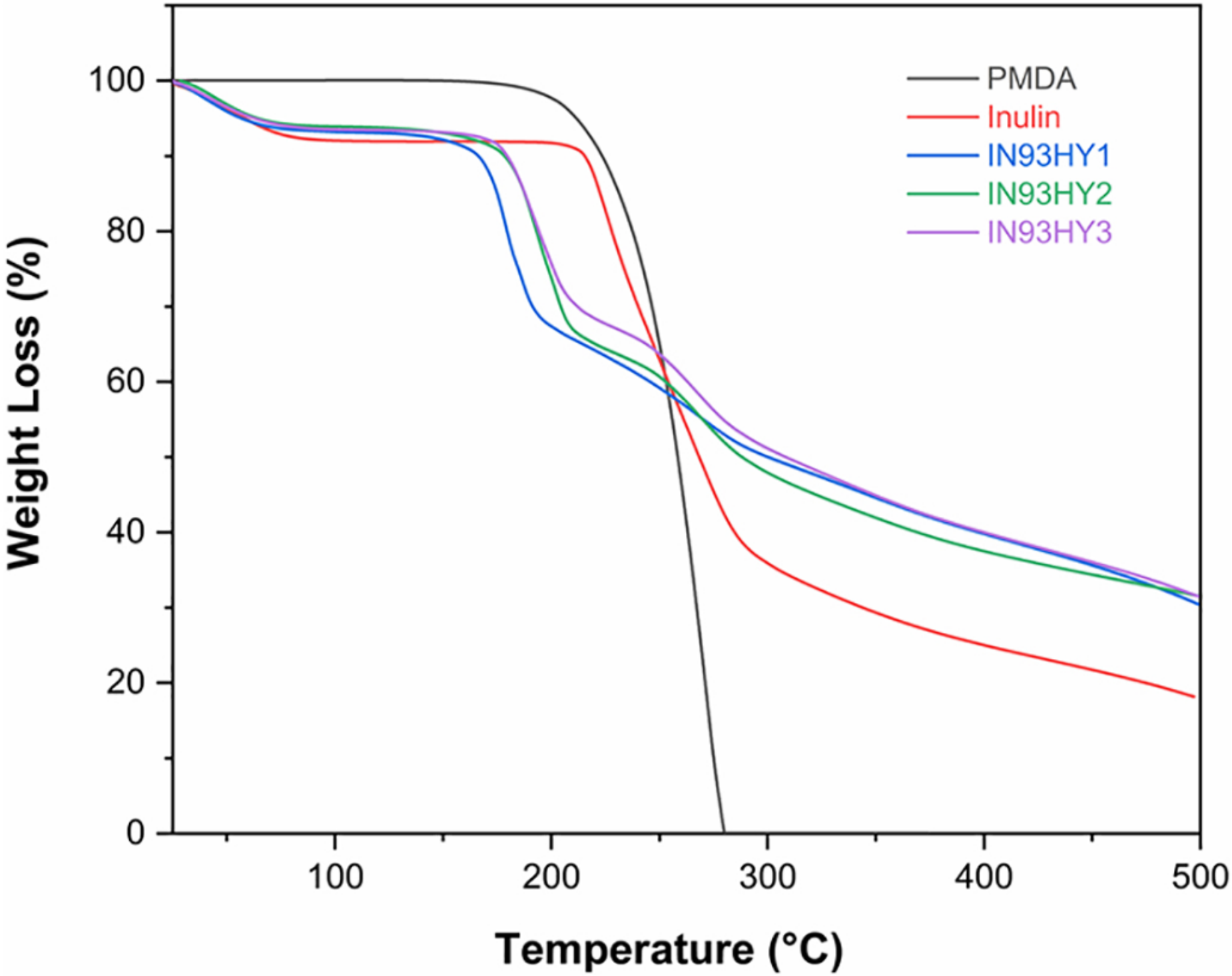
PMDA
Inulin
IN93HY1
IN93HY2
IN93HY3
Weight Loss (%)
100
80
60
40
20
0
100
200
300
400
500
Temperature (°C)

Figure 4

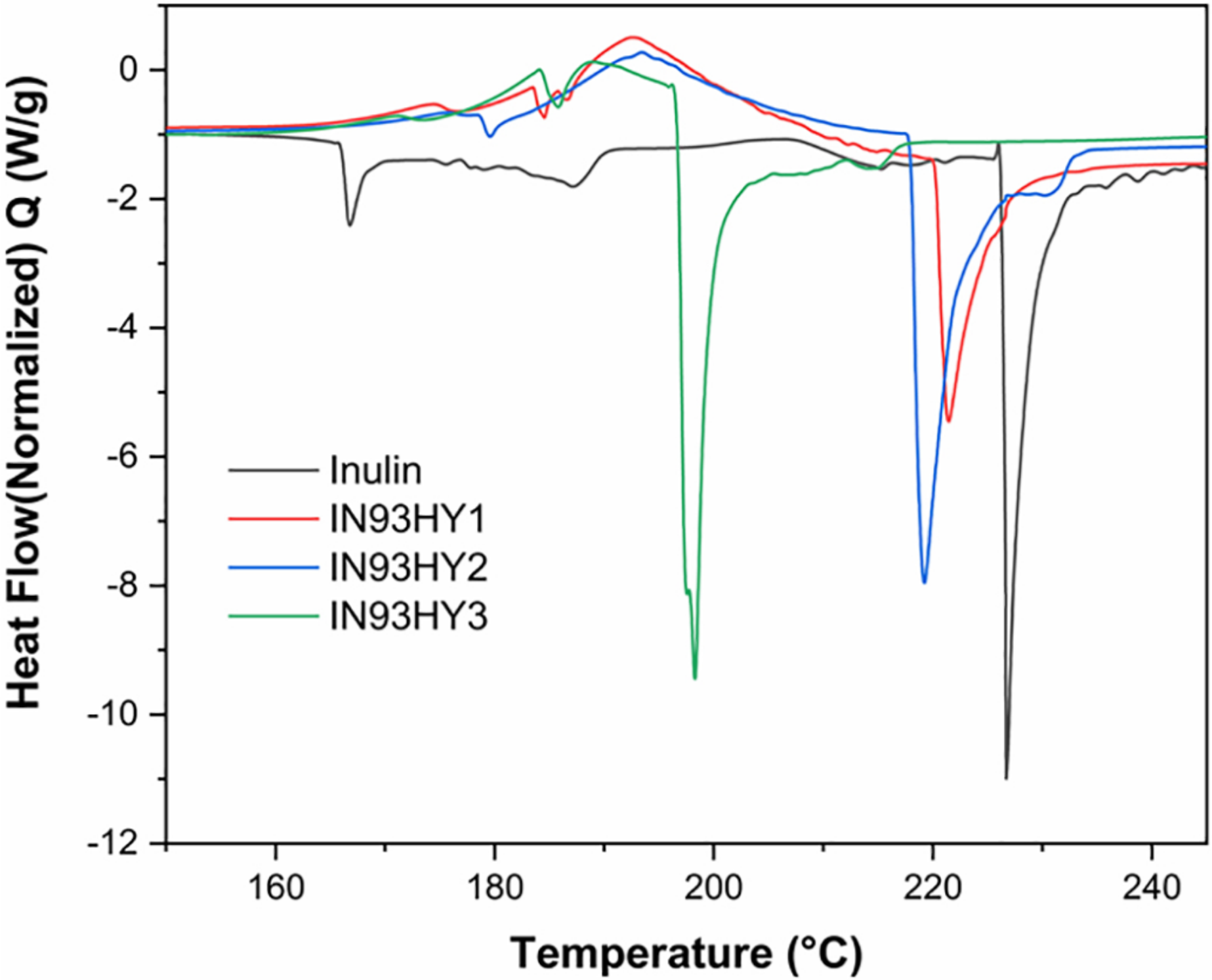
Heat Flow(Normalized) Q (W/g)
0
-2
-4
-6
-8
-10
-12
160
180
200
220
240
Temperature (°C)
Inulin
IN93HY1
IN93HY2
IN93HY3

Figure 5

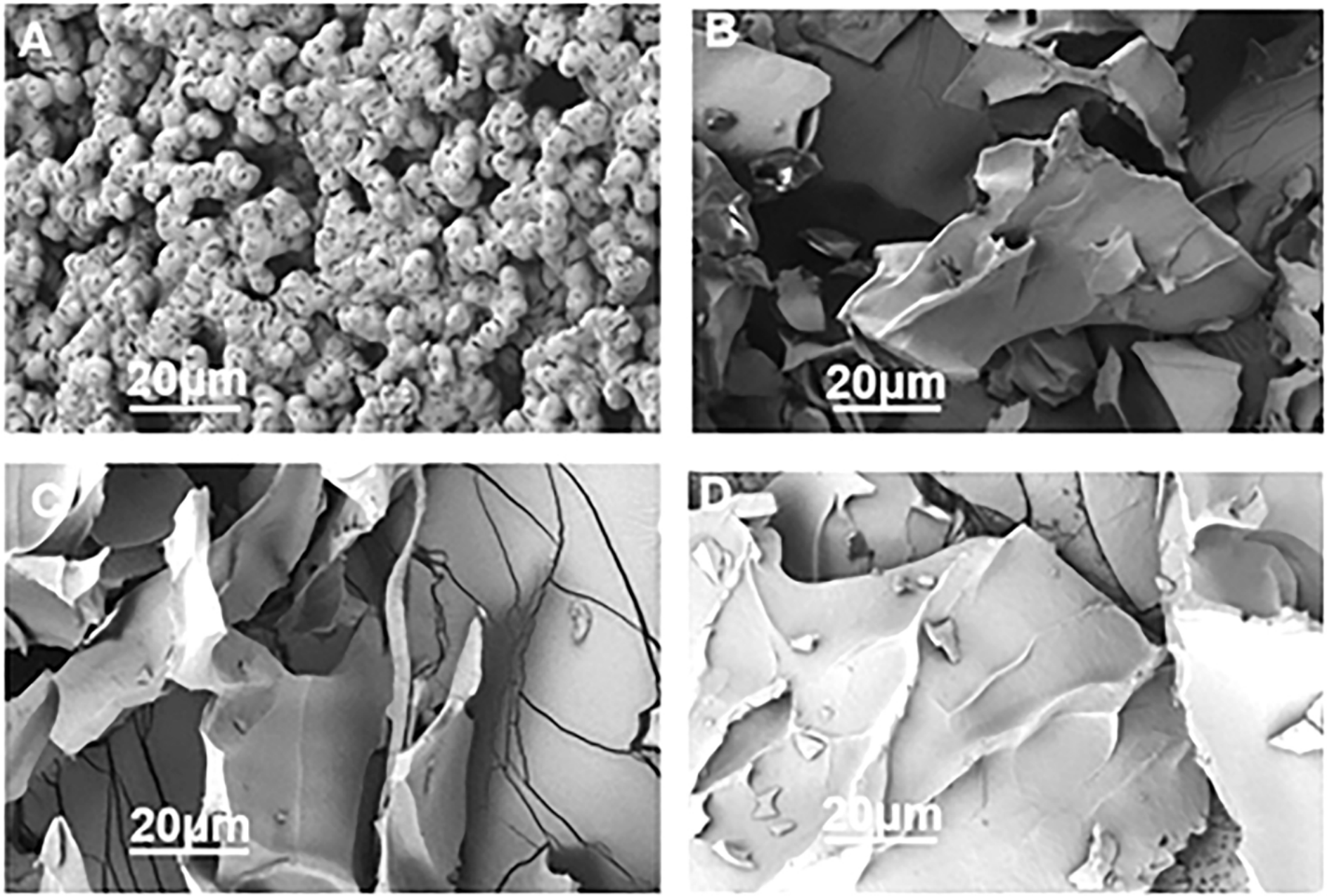

Figure 6

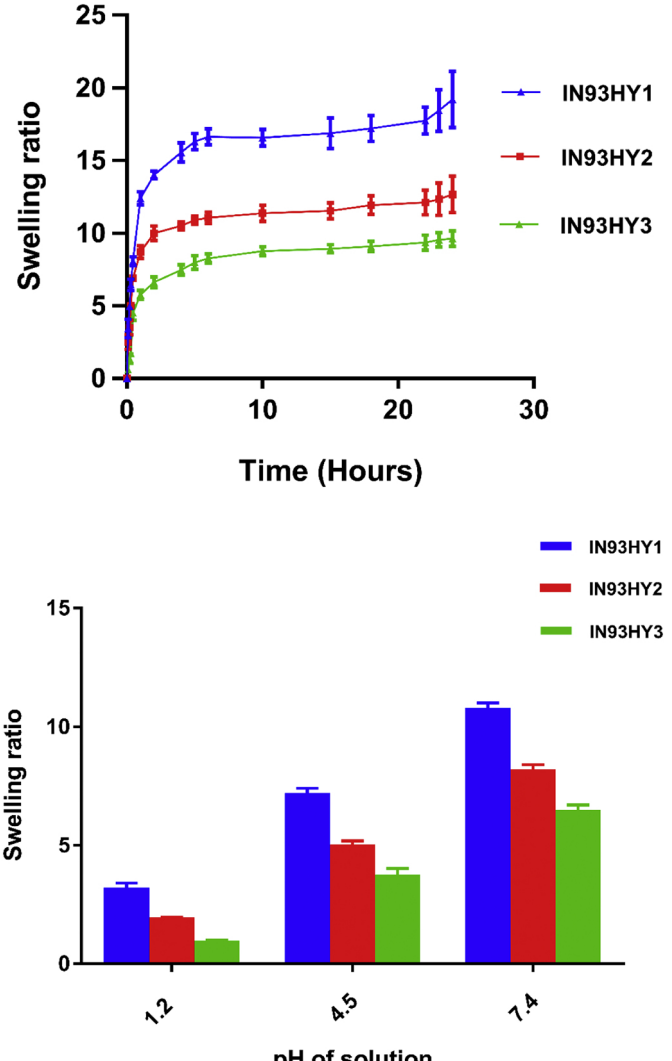
Swelling ratio
25
20
15
10
5
0
0
10
20
30
Time (Hours)
IN93HY1
IN93HY2
IN93HY3
Swelling ratio
15
10
5
0
1.2
4.5
7.4
pH of solution
IN93HY1
IN93HY2
IN93HY3

Figure 7